



Cite this: *Lab Chip*, 2017, **17**, 3760

Tumour-vessel-on-a-chip models for drug delivery

David Caballero, Sophie M. Blackburn,^a Mar de Pablo,^a Josep Samitier^{abc} and Lorenzo Albertazzi *^a

Nanocarriers for drug delivery have great potential to revolutionize cancer treatment, due to their enhanced selectivity and efficacy. Despite this great promise, researchers have had limited success in the clinical translation of this approach. One of the main causes of these difficulties is that standard *in vitro* models, typically used to understand nanocarriers' behaviour and screen their efficiency, do not provide the complexity typically encountered in living systems. In contrast, *in vivo* models, despite being highly physiological, display serious bottlenecks which threaten the relevancy of the obtained data. Microfluidics and nanofabrication can dramatically contribute to solving this issue, providing 3D high-throughput models with improved resemblance to *in vivo* systems. In particular, microfluidic models of tumour blood vessels can be used to better elucidate how new nanocarriers behave in the microcirculation of healthy and cancerous tissues. Several key steps of the drug delivery process such as extravasation, immune response and endothelial targeting happen under flow in capillaries and can be accurately modelled using microfluidics. In this review, we will present how tumour-vessel-on-a-chip systems can be used to investigate targeted drug delivery and which key factors need to be considered for the rational design of these materials. Future applications of this approach and its role in driving forward the next generation of targeted drug delivery methods will be discussed.

Received 29th May 2017,
Accepted 17th August 2017

DOI: 10.1039/c7lc00574a

rsc.li/loc

1. The drug delivery challenge and the potential of microfluidics

Microfluidic devices and organs-on-a-chip have had a dramatic impact on many fields of biomedicine.¹ These devices' parameters can be tightly controlled and they are not burdened by the cost and ethical concerns of animal models. Moreover, they present several advantages compared with classical 2D and 3D cell cultures, such as control over fluid and gas flows and chip architecture.² For these reasons, organs-on-a-chip are finding applications in the fields of drug discovery, regenerative medicine and nanomedicine.¹ Very few recent reviews have discussed the potential of organs-on-a-chip to help the field of nanomedicine and nanoparticle drug delivery.^{3–5} In this critical review, we will focus on vessel-on-a-chip models of the human vasculature to study and screen nanoparticles for drug delivery.

The development of nano-sized carriers for the selective delivery of therapeutics to the tumour site is one of the great challenges in material chemistry and nanotechnology.⁶ Despite some successful examples that are currently being used in the clinic such as Doxil®⁷ and Abraxane®,⁸ the field of



David Caballero

David Caballero holds a BS degree in Physics from the Autonomous University of Barcelona and MSc and PhD degrees in Nanoscience from the University of Barcelona (Barcelona, Spain). During his postdoctoral period at ISIS/IGBMC – University of Strasbourg (Strasbourg, France), he mainly worked on the biophysical description of directed cell migration using novel bioengineered approaches. Next, Dr. Caballero joined the Nano-bioengineering Group at IBEC led by Prof. Samitier to work in the field of 3D tumor models. In particular, Dr. Caballero's current research is focused on the development of a new generation of advanced organ-on-chip tumor models for future clinical applications.

^a Institute for Bioengineering of Catalonia (IBEC), The Barcelona Institute of Science and Technology, Baldiri Reixac 15-21, 08028 Barcelona, Spain.
E-mail: lalbertazzi@ibecbarcelona.eu

^b Department of Engineering: Electronics, University of Barcelona, 08028, Barcelona, Spain

^c Centro de Investigación Biomédica en Red en Bioingeniería, Biomateriales y Nanomedicina (CIBER-BBN), Madrid, Spain

† Current address: 3B's Research Group, University of Minho, Avepark – Parque de Ciência e Tecnologia, Zona Industrial da Gandra, 4805-017 Barco GMR, Portugal.

targeted drug delivery is far from harvesting the full potential of this approach. Recently, a critical review depicted the evolution of the performances of nanocarriers in cancer selectivity as reported in the literature.⁹ Strikingly, their targeting efficiency, *i.e.* the percentage of the injected dose that reaches the tumour, has not improved in the last 10 years and it is still lower than 1%.⁹ One of the main reasons is the limited knowledge about the behaviour of nanoparticles in the complex biological environment and the consequent difficulties of the materials' rational design. Moreover, the current models used to screen nanosystems are poorly predictive of the clinical output resulting in frequent failure in clinical trials. Microfluidics and nanofabrication can dramatically improve both of these aspects by providing a comprehensive and controlled system for the understanding and screening of nanocarriers for drug delivery. The behaviour of nanoparticles in the bloodstream is a major determinant of the

successful targeting of drug carriers as several key phenomena happen in blood vessels such as vascular targeting,¹⁰ margination,¹¹ extravasation,¹² protein corona formation,¹³ and immune system response (see Fig. 1).¹⁴

In this framework, the differences between tumour and healthy vasculatures are a main factor to be exploited by nanocarriers to achieve selective cancer accumulation. This extends beyond the well-known enhanced permeation and retention (EPR) effect:¹⁵ tumour vasculature displays a peculiar shape, unusual flow properties and different biochemical aspects of the endothelial cells.¹⁶ Understanding how to exploit these differences in order to design tumour-targeted nanoparticles is a key point of nanomedicine. Most of these features can be reproduced by vessel-on-a-chip models in a controlled and modular way.¹⁷

Here we discuss the design rules of vessels-on-a-chip as drug delivery models and provide an overview of the current



Sophie Blackburn

Sophie Blackburn is currently pursuing a BS degree in biological engineering at the Massachusetts Institute of Technology (Cambridge, MA). Her research interests focus on tissue engineering and the use of bio-printing for full scale organ development. She was able to join IBEC, thanks to a grant from the MIT International Science and Technology Initiatives (MISTI), and worked jointly with the Nanoscopy for Nanomedicine

Group led by Dr. Albertazzi and the Nanobioengineering Group led by Prof. Samitier.



Mar de Pablo

Mar de Pablo is currently pursuing the Degree of Medicine at Pompeu Fabra University (UPF) in Barcelona. In 2016, she received a scholarship to join the Nanobioengineering Group at IBEC led by Prof. Samitier. Her research interest is understanding and taking advantage of the differences between healthy and tumor microenvironments to create drugs that increase the life expectancy and life quality of cancer patients.



Josep Samitier

Josep Samitier is the Director of IBEC and a Full Professor in the Physics Faculty (Electronic Dep.), University of Barcelona. From February 1984 to June 1985 he was a visiting research fellow at the Philips Electronic Laboratory, Paris, France. From March 2001 to June 2005, Prof. Samitier was Deputy Head of the Barcelona Science Park (PCB), and in 2003 he received the Barcelona City Prize of the Barcelona Council in the area of

technology. Prof. Samitier is the coordinator of the Spanish Platform on Nanomedicine and the president of the Associació Catalana d'Entitats de Recerca (ACER).



Lorenzo Albertazzi

Lorenzo Albertazzi is Group Leader at the Institute for Bioengineering of Catalonia in Barcelona. He obtained his M.Sc. in Chemistry and PhD in Biophysics from Scuola Normale Superiore. After a short stay at the University of California Santa Barbara, he spent four years at the Eindhoven University of Technology as a postdoc. He moved to Barcelona in 2015 to start the Nanoscopy for Nanomedicine Group. For most of his

career he has been jumping between Chemistry and Biophysics; his group is now trying to combine them to achieve a molecular understanding of synthetic materials in the biological environment using advanced microscopy techniques.

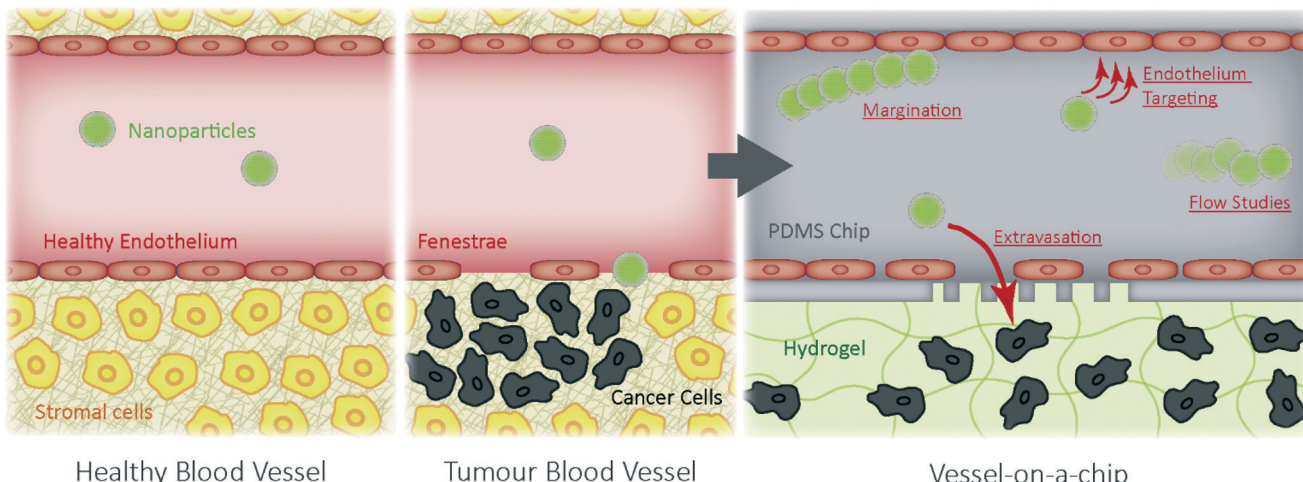


Fig. 1 Schematic displaying the applicability of nanoparticles (NPs) for cancer therapeutics. The perturbation of the vascular endothelium in tumour blood vessels can be exploited for directing drug-loaded NPs towards the tumor. Organ-on-chip models of blood vessels or blood vessels-on-a-chip can easily replicate the major components of the human vasculature and be used to study the behaviour of NPs under controlled flow conditions.

state-of-the-art in this field as well as future technological and scientific applications. We present a multidisciplinary perspective, taking into account blood vessel physiology, the necessity for therapeutic nanoparticles and the requirements for their development, and the most advanced fabrication methods. Only the integration of all of these disciplines will allow for the creation of devices which are able to provide fundamental contributions to nanomedicine for cancer therapies.

2. Physical and biochemical aspects of tumour capillaries and their microfluidic mimics

A crucial necessity for the development of an organ-on-a-chip model of a human blood vessel is the knowledge of the physical and biochemical cues of the *in vivo* scenario that we desire to mimic. Indeed, the growth of a tumour dramatically

impacts the structural and dynamical properties of blood vessels, inducing changes in their morphology, blood flow, oxygen distribution, pH, and others factors^{18,19} (see Table 1). Moreover, significant structural and functional heterogeneity has been shown among individual blood vessels within a single tumour and between different types of tumour, highlighting the complexity of the tumour microenvironment.¹⁸ A blood vessel model must therefore find a compromise between accurately representing the *in vivo* scenario and simplicity, cost-effectiveness, control and reproducibility. In this section, we describe the most relevant physicochemical differences between healthy and tumour vasculatures that can be captured by microfluidic devices.

Capillaries comprise the vast majority of the surface area of the circulation network and are the most relevant vessels for drug delivery, as they are the site of extravasation into the tumour tissue. While arterial walls are composed of three layers (endothelium, smooth muscle and fibrous tissue), capillaries display only a thin permeable wall and a microscopic

Table 1 Comparison of structural and functional properties between healthy and tumour human blood microvessels

	Healthy vessel	Tumour vessel	Consequence
Wall	Complete endothelium and basal membrane	Incomplete endothelium and basal membrane	Unstable flow, shunt perfusion, increased fragility
Geometry	Hierarchical and regular organization	Tortuous and irregular architecture	Cell sticking and aggregation, viscous resistance, altered flow
Density	Regular inter-capillary space	Chaotic network and spacing	Altered interstitial fluid flow and cell behaviour
Permeability	Continuous endothelium (<6 nm)	Leaky endothelium (100 nm–1 µm)	Favour intravasation of cancer cells and extravasation of NPs (EPR effect)
Diameter (µm)	5–25	15–50	Perturbation of blood flow and wall shear stress and rate
Blood flow (mL g ⁻¹ min ⁻¹)	0.2–0.5	0–1 (highly heterogeneous)	Non-functional vessels (up to 50%)
Shear stress (dyne per cm ²)	4	1–10 (highly heterogeneous)	The ability of lymphocytes to gain access to the tissue is perturbed
Endothelium biochemistry	Normal expression of endothelial markers	Endothelial genetic and metabolic dysfunctions	Overexpression of TEMs

lumen which connects the blood vessel to the surrounding tissue, *i.e.* the microcirculation. The endothelium of capillaries is typically continuous and has a vascular permeability of $<6\text{ nm}$,²⁰ with the exception of kidney and liver endothelia where *fenestrae* of about $0.1\text{--}1\text{ }\mu\text{m}$ are present to perform blood filtration.²¹ The microcirculation is completely different from tumour vasculature which often presents large gaps in the vessel walls (see Fig. 2 and Table 1).²² The occurrence and size of such openings can vary; however, typical pore sizes range from 100 nm to $1\text{ }\mu\text{m}$.²³ Moreover, tumour blood vessels usually have a defective or entirely absent basal membrane. These phenomena result in increased vessel permeability of nanoparticles (NPs), described as the EPR effect, which can be exploited for the passive targeting of drug carriers.²⁴ However, the heterogeneity and complexity of this phenomenon makes the rational design of nanoparticles challenging. Recent examples are the issues encountered during clinical trials using Bind014, a PLGA-based NP for prostate cancer therapy, which were mainly attributed to the heterogeneity of the EPR effect among patients.^{25,26} Microfluidic models with varying *fenestrae* size and distribution of endothelium²⁷ would provide valuable information about the ideal nanoparticle properties (*e.g.* size) that maximize passive tumour targeting and help screen new NPs more accurately.

Due to differences in the endothelium *fenestrae*, the size and geometry of capillaries change dramatically in the tumour tissue. Intravital microscopy allows for the visualization of abnormalities in the capillary diameter (larger than $30\text{ }\mu\text{m}$ (ref. 28)) in both pre-clinical models²⁹ and cancer patients.³⁰ Tumour vessels also exhibit typical behaviour, such as branching off, overlapping, being disorganized, and having tortuous vases (see Table 1 and Fig. 2). This altered geometry results in dramatic differences in the blood flow and up to 50% of vessels being non-functional.³⁰ These characteristics can be exploited to develop targeted nanoparticles that exhibit enhanced affinity under these peculiar flow conditions.

Vessels-on-a-chip are an ideal model to study such a phenomenon as they allow for the creation of vessel-like channels with arbitrary sizes and geometries allowing to reproduce the exact pathological geometry of the tumour vasculature from an *in vivo* image.³¹

In addition to their physical differences, the biochemistry of tumour endothelium is profoundly different from that of healthy vasculature. Factors such as hypoxia and chronic growth factor stimulation result in genetic and metabolic dysfunctions. These factors have led to the identification of tumour endothelial markers (TEMs), *i.e.* membrane proteins that are overexpressed in the tumour vessels compared to the healthy ones.³² In a pioneering report, St Croix and co-workers performed a gene expression profiling of tumoural endothelial cells and found 46 transcripts that were overexpressed in colorectal cancer cells.³³ This approach has been replicated for other types of cancers including glioma,³⁴ ovarian cancer,³⁵ and breast cancer.³⁶ Interestingly, the TEMs found are tumour specific; every cancer type has a different impact on the endothelium's biochemistry. Several TEMs are overexpressed 10-fold in tumour vasculature compared with healthy tissues. These include membrane receptors such as CD276, CD137, MIRP2, PTPRN, and CD109.³⁷ This paves the way towards the development of homing peptides for selective tumour vascular targeting. The ability to isolate and expand tumoural endothelial cells within microfluidic devices will permit the development of an accurate, even personalized, model of tumour endothelium that can be used to screen drug carriers targeting specific membrane receptors.

3. How to build a vessel-on-a-chip

Extensive research has been performed during the past few years aimed at developing microfluidic blood vessel-like devices for a plethora of applications. The large diversity in blood vessel sizes requires the use of different fabrication technologies to recreate *in vivo*-like vasculature structures, as recently reviewed³⁸ (see Fig. 3). In the following section, we briefly describe the main microfabrication technologies typically used for the development of microfluidic networks with architectural features reminiscent of vasculature.

3.1 Microfluidics-based devices

Microfluidic-based devices are typically fabricated in a polymeric material such as polydimethylsiloxane (PDMS) replicated from a master, usually fabricated by standard UV or laser-assisted photolithography. This approach permits the fabrication of structures in the range of about $1\text{--}5\text{ }\mu\text{m}$ in lateral resolution and up to $200\text{ }\mu\text{m}$ in thickness. Besides the limit of resolution intrinsic of micro and nanotechnology, there is an additional limitation of this methodology: the use of small microfabricated vessels results in elevated fluid friction which makes it difficult to supply cells with sufficient nutrients. A variety of microfluidic-based models of blood vessels have been developed.³⁸ They differ in their design and complexity, ranging from simple hollow polymeric

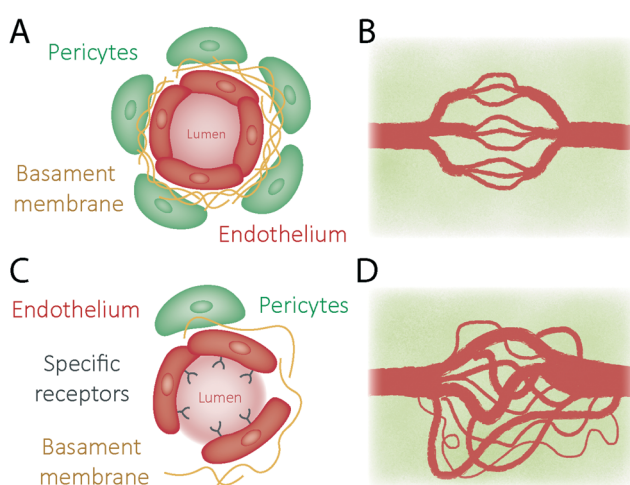


Fig. 2 Schematic representation of the difference in structure (A–C) and geometry (B–D) between healthy (top) and tumour (bottom) vessels.

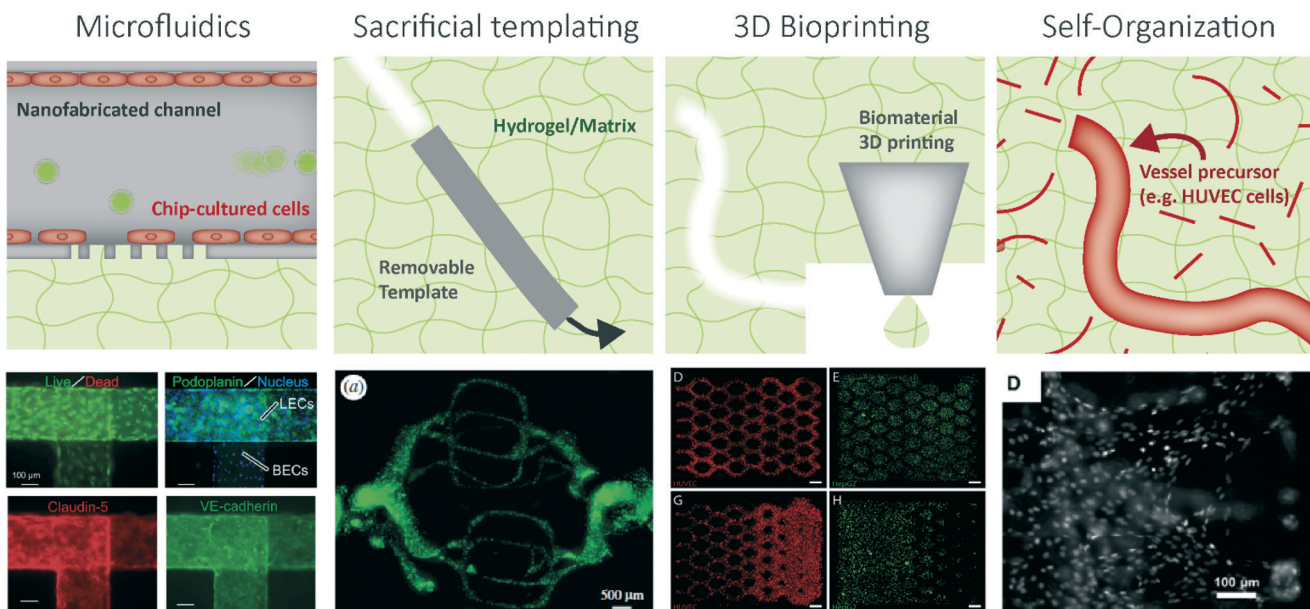


Fig. 3 Typical fabrication methods of organ-on-a-chip models of human blood-vessels. (Upper) Scheme and (Lower) examples displaying the most frequent fabrication techniques of blood vessel models. Left: Microfluidics-based chip. The example shows microfabricated channels where blood vessels' endothelial cells (red) and lymphatic endothelial cells (green) are cultured.⁴¹ Middle-left: Sacrificial templating. The example shows HUVEC cells (green) populating channels obtained by sacrificial templating inside a fibrin gel.⁴⁶ Middle-right: 3D (bio)printing. The example shows the co-culture of HUVEC (red) and HepG2 (green) cells into a 3D-printed structure.⁵¹ Right: Self-organization. The example shows nuclear staining of HUVEC cells self-organized into a network structure after 4 days of culture into a fibrin gel.⁵⁸ Lower images reproduced with permission from references.

channels coated with endothelial cells, to devices incorporating porous PDMS membranes, or 3D cavities filled with an ECM protein. Hollow channels permit the study of shear stress effects on NP interactions with cells using simple straight channels³⁹ or a geometry similar to that of an *in vivo* microvascular network.⁴⁰ In addition, porous membranes can be used to separate the vessel-like channel from a secondary channel containing the cells of interest to study the permeability of chemical compounds, NPs, or other cell types. A good example is a microfluidic model of the human microcirculation system containing both blood and lymphatic vessels which was recently developed⁴¹ (see Fig. 3). In this model, a porous PDMS membrane separated the cell-containing blood vessel channels from the lymphatic ones. Interestingly, the model recapitulated *in vivo*-like responses, such as enhanced vessel permeability upon induced inflammation. Finally, confined ECM-derived gels permit similar studies in a 3D-like microenvironment, together with vascularization studies. All of these methods permit high control over the mechanical and biochemical properties of the model. In addition, they support the generation of biochemical gradients to reproduce physiopathological events, such as cancer cell invasion into the microcirculation system.⁴²

Control over the perfusion of microfluidic devices is an important parameter to consider if intending to mimic the hydrodynamic properties of human blood vessels, nutrient supply, waste removal, or the delivery of drug compounds to cells. The selection of the perfusion system depends on the desired parameters, such as controlled or non-controlled

fluid flow, perfusion rate, shear stress, or fluid recirculation. Different types of pumping devices are typically used to allow fluids to flow through microfluidic chips in a controlled manner, namely pneumatic pressure-driven, syringe, or peristaltic pumps. Pneumatic pumps allow for high control and stable fluid flow in contrast to syringe pumps, which display some fluctuations in fluid flow at low flow rates. In addition, syringe pumps suffer from a significant delay in flow rate variation. Similarly, peristaltic pumps, albeit simple, are not capable of generating stable flow rates due to their reliance on moving mechanical parts. On the other hand, they show an elevated level of miniaturization capability. Other more sophisticated pumps have also been described, such as a stirrer-based pump actuated by an external magnet, or micro-pumps actuated by an electroosmotic mechanism.⁴³ However, these pumping mechanisms are limited to the specific needs of the final user and may affect the physiology of the cells. Finally, fluid flow driven by gravitational force displays several advantages. This method is simple and shows an immediate change of flow upon variation of height. Unfortunately, precise control of the fluid levels is difficult.

3.2 Sacrificial templating

Sacrificial templating involves the use of a sacrificial structure to cast a synthetic or ECM-based material.^{44,45} The resulting hollow channels can then be filled with endothelial cells and cell culture media. Typically, channels with a diameter of around 100 µm can be fabricated and incorporated

within a microfluidic device to mimic a blood vessel. This fabrication method overcomes the limitations of solid polymeric channels, where the activity is restricted, in general, to the inner part of the channel. In this case, the ECM-like gel allows the study of multiple cellular phenomena, including vascularization, intravasation, or permeability. Further, the mechanical properties and composition of the gel can be easily controlled to study its effect on endothelial cell response. Unfortunately, sacrificial templating is generally limited to uniaxial-patterned channels and has poor spatial resolution. However, 3D-like structures can also be obtained. For example, a hierarchical 3D vascular network coated with endothelial cells using a fibrin hydrogel was recently developed by means of sacrificial templating⁴⁶ (see Fig. 3). This model was highly perfusable; it contained multi-sized bifurcating channels, which ranged from 200 µm to 1 mm. Additionally, it was found to have high cell viability and demonstrated cellular responses typically observed *in vivo*. A variation of the sacrificial templating method uses *removable mandrels* to create small blood models. Cells are cultured around polymer strands to mimic the morphology of blood vessels. The strands are then mechanically removed to liberate the vessels.⁴⁷ It is important to note that the resulting vessels can then be integrated within a microfluidic device and connected to perfusion channels, which could be used to flow and seed endothelial cells. An ECM can be cast around the vessels to provide them with both mechanical support and biochemical stimuli. Using this approach, an angiogenesis model was created with two parallel perfused channels fabricated from collagen, incorporating pericytes. One of the channels was used to create a gradient of the vascular endothelial growth factor which induced the sprouting of endothelial cells from the other channel and the recruitment of pericytes around the vessels, thus replicating angiogenesis *in vitro*.⁴⁸

3.3 3D (bio)printing

Fabrication of vascular networks with 3D (bio)printing overcomes many of the limitations of the above-mentioned techniques.^{49,50} The printing process is fast, controllable, and in general, inexpensive. Cells can be directly printed into the device or can be seeded at a later stage. Three-dimensional complex architectures can be easily fabricated using different types of (bio)materials,⁴⁹ including polymers, natural and synthetic hydrogels, or cells. The family of 3D (bio)printing includes a diverse variety of techniques, including *inkjet deposition*, *extrusion*, and *stereolithography*. Inkjet deposition dispenses biomaterials, such as cells, or cells deposited in a dissolvable matrix precursor (*e.g.* gelatin) or initiator (*e.g.* calcium chloride), layer-by-layer to print 3D structures, such as cylindrical blood vessels. Similarly, the extrusion method dispenses a material, typically a thermoresistive polymer, through an extruder. Sacrificial extruded templates are typically used to support the adhesion of cells. Finally, stereolithography uses a raster scan laser or projected light (typi-

cally UV – 365 nm) to generate structures by photopolymerizing a liquid photosensitive material layer-by-layer in a photochemical reaction. In this case, resolution is determined by the laser spot size or projector pixel size. Recently, a UV LED was used to reproduce the branching structure of a vasculature network using photopolymerizable hydrogels⁵¹ (see Fig. 3). The bioprinted vasculature model displayed good cell viability and high control on the morphology of complex channels. Notably, a high-resolution model of a native capillary network was replicated from an *in vivo* image, demonstrating the capabilities of this technique.

3D (bio)printing can be used for the fabrication of mm-sized vasculatures. However, spatial resolution is still limited, in general, to structures with feature sizes of around 100 µm, which might limit the applicability of this technique to the fabrication of small capillaries.⁵² This limit of resolution can be overcome by stimulating angiogenesis to obtain vessels of 10–20 µm in diameter, or using related bioprinting techniques, such as *laser-assisted bioprinting*. This technique uses a 10 ms pulse laser to transfer, following a pre-defined CAD design, the content of a *bio-ink* cartridge (containing cells or the biomaterial of interest) onto the so-called *bio-paper*. This technique is fast, flexible, and high-throughput. Resolution is determined by the size of the laminar fluid jet which is formed after the laser pulse and can reach cell- or picolitre-levels of resolution.⁵³ In summary, 3D (bio)printing is intended to be used for the fabrication of large vascular structures. For a detailed review on the use of 3D (bio)printing for the fabrication of vasculature networks, readers are referred to references.^{49,50}

3.4 Self-organization

The self-organization fabrication strategy induces vasculogenesis or angiogenesis of endothelial cells. Typically, microfluidic devices are used to promote the guided growth of newly formed vasculature by means of pressure/chemical gradients.⁵⁴ Typically, an ECM-based solution containing endothelial cells is injected into a microfluidic channel connected to two lateral channels by micro-sized posts. The lateral channels are used to supply nutrients and pro-angiogenic agents to cells once the gel hardens. Even though vasculogenesis and angiogenesis allow endothelial cells to form vessels naturally, only minimal control over their growth, both spatially and temporally, can be obtained. The self-organization can produce vessels with diameters of around 10–100 µm and take up to 7 days. Many *in vivo*-like behaviours have been reproduced by means of vasculature self-organization, including the production of adherent junction proteins, continuous cell-cell junctions, elongated endothelial cells in the direction of the capillary, and F-actin rearrangement and increased production of nitric oxide under shear stress. Unfortunately, the growth of a fully perfusible network cannot be guaranteed.^{55,56} Microfluidic devices can, nevertheless, provide improved

spatiotemporal control over vasculogenesis/angiogenesis. For example, vasculogenesis was induced in the centre of a microfluidic device containing a tissue chamber to mimic native capillaries. Adjacent microfluidic channels were lined with a monolayer of endothelial cells to mimic an artery and a vein.⁵⁷ The proliferation of endothelial cells was then induced bidirectionally between the microchannels and the tissue chamber. This work established a physiological transport model of interconnected perfused vessels from an artery to vascularized tissue to a vein, and offered a large spectrum of applications based on organ-on-a-chip technology. However, some limitations were observed, such as the lack of smooth muscle cell coverage to regulate vasoconstriction and the formation of microvessels that were larger than typical *in vivo* capillaries. Similarly, a microvessel-on-a-chip device that mimic the *in vivo* capillary bed was recently developed for the study of targeted drug delivery⁵⁴ (see Fig. 3). Human umbilical vein endothelial cells (HUVEC) and lung fibroblasts were seeded in the central and lateral channels of a multi-channel microfluidic device, respectively. The cytokines released by the fibroblasts then directed the formation and growth of perfusable vessels. This platform demonstrated great promise to be used as a drug screening model.

4. Microfluidics and drug delivery

Several microfluidic devices describing, or predicting, the behaviour of nanocarriers *in vivo* have been described in the literature. These studies aim to understand the behaviour of nanoparticles in the blood with a specific focus on their ability to selectively extravasate and accumulate in the tumour site. Several crucial phenomena such as vascular targeting, the EPR effect, protein corona formation, and immune clearance, have been studied in controlled vessel-on-a-chip

models, providing crucial information for the design of the next generation of targeted nanoparticles.

4.1 Vascular targeting

As previously mentioned, the endothelium of tumour tissues displays several unique features that can be exploited for selective – vascular – targeting (see Fig. 4A). However, achieving a selective and effective recognition of pathological endothelium under flow is highly challenging and is prone to causing vascular damage which leads to serious side effects.⁵⁹ The impact of physiological parameters, such as vessel geometry and shear stress, in relation to particle properties, such as size, has been characterized using microfluidic devices.⁶⁰ Shear stress plays a pivotal role in the binding of nanoparticles to the endothelial surface as it dramatically alters the cells' ability to perform particle uptake by endocytosis.⁶¹ Interestingly, it has been recently reported that although flow adaptation reduces the cell uptake of non-targeted gold NPs, it enhances the uptake of ICAM-1 targeted NPs.⁶² Therefore, shear stress can potentially be used to enhance vascular targeting. In this regard, a shear-responsive carrier was developed using a vessel-on-a-chip model, which mimicked the shear effects of pathological sites and constricted vessels.⁶³ This large shear-responsive particle took advantage of sites with high shear stress to disassemble into smaller NPs with enhanced cell internalization. This concept can be used to target drugs selectively to sites of flow obstruction. Microfluidic models of blood vessels have been fundamental to prove that, not only the size and functionalization but also the particle shape is critical in vascular targeting. Indeed, several examples of shape-dependent endothelium targeting have been reported using microfluidic devices with different geometries.^{64,65} Their results highlighted the enhanced targeting of elongated rod-

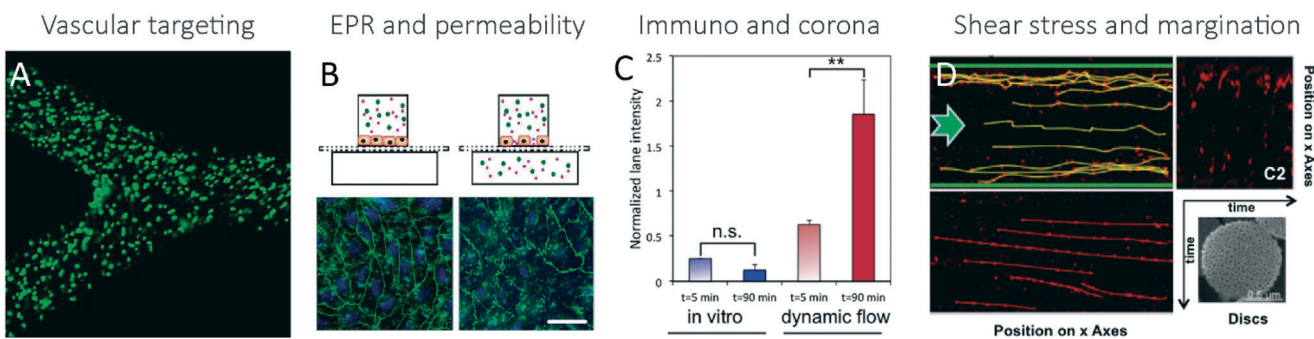


Fig. 4 Vessel-on-a-chip models for the characterization of the behaviour of nanoparticles in the microcirculation system. The morphological and molecular characteristics of – tumoural – blood vessels, together with the physicochemical properties that nanoparticles display under flow, can be exploited to improve the transport and delivery of drug-loaded carriers towards the region of interest. In this regard, models of A vascular targeting,⁷⁹ B EPR and permeability,⁸⁰ C corona formation and immune clearance,⁸¹ and D margination have been successfully developed.⁸² Reproduced with permission from the references. A) Confocal imaging of 210 nm nanoparticles targeting ICAM-1 coated surfaces of a microfluidic chip. B) Confocal imaging of cadherin junctions of endothelial cells forming a perfect monolayer (left) and a permeable one (right). C) Histogram showing the amount of protein adsorbed on liposomes under static conditions and under flow highlighting the effect of shear stress on protein corona formation. D) Particle trajectories (yellow) for 500 nm nanodisks obtained by intravital microscopy highlighting the margination effect due to the interactions with blood cells.

like structures, thanks to their high surface area and lower flow drag.

4.2 EPR and permeability

An alternative to active vascular targeting is to take advantage of the leakiness associated with the endothelium of several diseased tissues, better known as the EPR effect (see Fig. 4B). Despite being currently exploited by clinically-approved nanocarriers, the variability in size and shape of the *fenestrae* between tumours and even between vessels of the same tumour poses a serious challenge to the design of passive-targeted NPs. Within this framework, vessels-on-a-chip models have been used to understand the design rules for carriers that exploit endothelium permeability. A microfluidic model of a vascular network with controllable permeability was developed to study lipidic nanoparticle translocation.⁶⁶ Trans-epithelial electrical resistance measurements showed an increase in nanoparticle translocation for larger permeability values. These results were further validated *in vivo* using a rabbit model of atherosclerosis to confirm the applicability of the microfluidic model. Additionally, a tumour microvasculature model with *in vivo*-like geometry and variable permeability was recently used to study GFP gene delivery efficiency. The device reproduced the transport of nanoparticles across leaky vessel walls using spheroids of HeLa cells on microfluidic channels coated with endothelial cells. Two nano-polymer gene delivery systems were tested and it was demonstrated that the device accurately represented the carrier's *in vivo* behaviour.⁶⁷ Similarly, the relationship between vessel permeability and the accumulation of NPs in the tumour was investigated using a tumour-on-a-chip model. Furthermore, the interaction between nanocarriers and tumour spheroids has been monitored under physiological flow conditions.⁶⁸ Results showed that the penetration of nanocarriers into the tissue was mediated by their size and receptor interactions. Interestingly, an increased flow rate induced an increase in drug accumulation in the tumour. Most importantly, these findings were confirmed using an *in vivo* murine tumour model.

4.3 Protein corona and immune clearance

Two key phenomena of nanoparticle delivery that occurs in the bloodstream is the formation of a protein corona and the immunogenicity of NPs. These two related events are responsible for the clearance of synthetic nanostructures from the circulation which result in poor NP efficiency and toxicity. The adhesion of serum proteins to the nanoparticle's surface forms a biomolecular corona that may modify the NP's physicochemical properties and targeting affinity. This phenomenon has been extensively studied *in vitro* under static conditions.¹³ However, the flow and shear stress present *in vivo* can dramatically modify the protein binding and therefore the corona composition. Recent studies have demonstrated using microfluidics that the composition of the protein corona is significantly different under flow. In particular, spe-

cific proteins have been found in the corona formed "under flow" that were not present in the "static" one. In addition, some protein species were less enriched in the microfluidic experiment.⁶⁹ This is very relevant with regard to the *in vivo* fate of NPs. Under dynamic conditions, they display a corona which is less enriched in complement proteins, a main signal to the immune system, which will result in reduced immunogenicity and toxicity. Moreover, it has been demonstrated that the effect of shear stress on corona composition has an impact on its ability to be internalized by different cancer cell lines.⁷⁰ The use of a microfluidic model, in contrast to an *in vivo* animal experiment, allows for control over the composition of the blood used, permitting the use of human blood and even blood from cancer patients. This is of crucial importance as it has been shown that serum from different animals displays a different protein adsorption pattern.⁷¹ Finally, the combination of microfluidic chips and surface plasmon resonance provides detailed information about the kinematics of corona formation. In this regard, a microfluidic device containing immobilized NPs and flowing proteins was able to monitor the interaction of nanoparticles with serum proteins in real time.⁷² This allowed for the quantitative measurement of different binding affinities (k_{on} and k_{off}).

Phagocytosis of nanocarriers by the immune system limits the ability of nanocarriers to selectively target specific sites. In order to better understand the immune clearance of nanocarriers, microfluidic models mimicking the key organ functions involved were recently developed. For example, a splenon-on-a-chip was developed to study the hydrodynamics of blood flow.⁷³ In this work, enhanced accumulation of old, rigid and malaria-infected RBCs was observed on micro-slits with constraints designed to mimic *in vivo* spleen filtering properties. *In vivo*, this physical trapping facilitates the recognition and destruction of unhealthy RBCs by specialized macrophages, confirming the physiological relevance of the microfluidic model. This work supported the observed accumulation of big, rigid nanoparticles in the spleen and could provide key insights into the development of novel nanocarriers with reduced organ accumulation. Similarly, a liver-on-a-chip model was developed which mimicked the functional characteristics of the human liver.⁷⁴ In this work, a 3D liver organoid was embedded inside of a perfused microfluidic device. This multicellular model included macrophages to mimic the liver's immune response to infection. Importantly, the developed model displayed certain morphological and functional similarities to the *in vivo* scenario, confirming the potential applicability of the model to the study of liver-related physiopathological phenomena.

4.4 Margination

In order to extravasate into the tumour tissues, it is crucial that the NPs flowing in a blood vessel can approach the lateral side of the vessel and interact with the endothelial layer. Several effects can contribute to the migration of nanoparticles towards the vessel wall, also known as

margination. This phenomenon occurs with various blood components, such as platelets, and is mostly attributed to the collision with bulky red blood cells that scatter the platelets toward the side of the vessel.⁷⁵ In the same way, margination can influence nano- and micro-particles playing a role in their extravasation ability.⁷⁶ A combination of microfluidics and single particle tracking revealed a strong margination effect on drug carriers that is dependent on particle size and shape.⁷⁷ Interestingly, it was found that the most efficient geometry for margination was the discoidal one, with a shape analogous to that of platelets. There was a strong correlation between an increased margination effect and the enhanced *in vivo* extravasation of these disc-like particles. Dense silica and titania nanoparticles showed enhanced near-wall localization due to gravity and centrifugal forces during flow.⁷⁸ This highlights the improved vascular targeting of dense particles compared with their more buoyant counterpart.

5. Future perspectives

Despite vessel-on-a-chip devices having already significantly contributed to the drug delivery field, we envision several exciting future perspectives. A main development will be the design of devices with increased complexity. Two directions can be foreseen: i) the creation of microfluidic chips where multiple cell types (tumour, endothelial, stem, tumour-associate macrophages, and fibroblasts) and compartments are incorporated and ii) the connection of different devices in series to mimic the different tissues (*e.g.* liver, spleen, tumour) that play a role in targeted drug delivery, *i.e.* body-on-a-chip.⁸³ The design of such complex devices is clearly attractive; however, complexity comes with a price in terms of reproducibility and cost that should be taken into account. We must find a compromise between simplicity and control *versus* biomimicry.

A second very interesting perspective is the development of microfluidic devices that incorporate patients' cells, tissues or fluids (*e.g.* blood and cancer cells from biopsies). This would better mimic the clinical *in vivo* setting and contribute to the growing field of personalized medicine.⁸⁴

The integration of vessels-on-a-chip with other technologies will be a crucial step towards the understanding of nanoparticle structure–activity relations. In this framework, the combination of microfluidics and advanced microscopy will play a pivotal role. Novel and exciting techniques such as super resolution microscopy⁸⁵ and light-sheet microscopy⁸⁶ are emerging as tools to obtain unprecedented details of biological samples on multiple scales. Therefore, the combination of nanotechnology, microfluidics, and advanced microscopy holds great promise to unveiling the hidden molecular interactions that prevent the rational design of nanomedicines.

The advanced organ-on-a-chip models described above will undoubtedly boost the commercial potential of such devices. In this regard, the US Food and Drug Administration has recently started using organ-on-a-chip technology to model the

response of the human liver to food and food-borne illnesses.⁸⁷ This liver-on-a-chip model may help assess the toxicity of food additives and compounds to reduce animal testing. We envision similar future applications for organs-on-a-chip in the nanomedicine and drug delivery markets. To ensure the adoption of these technologies by a wide range of users, it is crucial that they are easy to manipulate, high-throughput, reproducible, and integrated with complementary analytical tools.⁸⁸ In this framework, the collaboration and the knowledge-exchange between (bio)engineers, biologists, chemists, physicians and pharmaceutical companies to successfully develop and employ microfluidics-based tumour models will be crucial.

Conflicts of interest

There are no conflicts to declare.

Acknowledgements

This work was financially supported by the AXA Research Fund (L. A.), the Spanish Ministry of Economy, Industry and Competitiveness through the Centro de Excelencia Severo Ochoa Award, and the Generalitat de Catalunya through the CERCA program. Moreover, this work was supported by the Spanish Ministry of Economy and Competitiveness through the project SAF2016-75241-R (MINECO/FEDER). The Nano-bioengineering SIC-BIO Group is supported by the Commission for Universities and Research of the Department of Innovation, Universities, and Enterprise of the Generalitat de Catalunya (2014 SGR 1442). This work was partially supported by the project MINDS (TEC2015-70104-P), awarded by the Spanish Ministry of Economy and Competitiveness. D. C. acknowledges the support of the Secretary for Universities and Research of the Ministry of Economy and Knowledge of the Government of Catalonia and the COFUND program of the Marie Curie Actions of the 7th R&D Framework Program of the European Union (2013 BP_B 00103). This work was supported by the Networking Biomedical Research Center (CIBER), Spain. CIBER is an initiative funded by the VI National R&D&I Plan 2008–2011, Iniciativa Ingenio 2010, Consolider Program, CIBER Actions, and the Instituto de Salud Carlos III, with the support of the European Regional Development Fund.

References

- 1 S. N. Bhatia and D. E. Ingber, *Nat. Biotechnol.*, 2014, 32, 760–772.
- 2 D. Huh, B. D. Matthews, A. Mammoto, M. Montoya-Zavala, H. Y. Hsin and D. E. Ingber, *Science*, 2010, 328, 1662–1668.
- 3 Y. S. Zhang, Y.-N. Zhang and W. Zhang, *Drug Discovery Today*, DOI: 10.1016/j.drudis.2017.03.011.
- 4 A. Ozcelikkale, H.-R. Moon, M. Linnes and B. Han, *Wiley Interdiscip. Rev.: Nanomed. Nanobiotechnol.*, 2017, 9(5), DOI: 10.1002/wnan.1460.

- 5 N. S. Bhise, J. Ribas, V. Manoharan, Y. S. Zhang, A. Polini, S. Massa, M. R. Dokmeci and A. Khademhosseini, *J. Controlled Release*, 2014, **190**, 82–93.
- 6 M. W. Tibbitt, J. E. Dahlman and R. Langer, *J. Am. Chem. Soc.*, 2016, **138**(3), 704–717.
- 7 Y. (Chezy) Barenholz, *J. Controlled Release*, 2012, **160**, 117–134.
- 8 E. Miele, G. P. Spinelli, E. Miele, F. Tomao and S. Tomao, *Int. J. Nanomed.*, 2009, **4**, 99–105.
- 9 S. Wilhelm, A. J. Tavares, Q. Dai, S. Ohta, J. Audet, H. F. Dvorak and W. C. W. Chan, *Nat. Rev. Mater.*, 2016, **1**, 16014.
- 10 D. Neri and R. Bicknell, *Nat. Rev. Cancer*, 2005, **5**, 436–446.
- 11 F. Gentile, A. Curcio, C. Indolfi, M. Ferrari and P. Decuzzi, *J. Nanobiotechnol.*, 2008, **6**, 9.
- 12 E. Blanco, H. Shen and M. Ferrari, *Nat. Biotechnol.*, 2015, **33**, 941–951.
- 13 M. P. Monopoli, C. Åberg, A. Salvati and K. A. Dawson, *Nat. Nanotechnol.*, 2012, **7**, 779–786.
- 14 D. F. Moyano, M. Goldsmith, D. J. Solfield, D. Landesman-Milo, O. R. Miranda, D. Peer and V. M. Rotello, *J. Am. Chem. Soc.*, 2012, **134**, 3965–3967.
- 15 H. Hashizume, P. Baluk, S. Morikawa, J. W. McLean, G. Thurston, S. Roberge, R. K. Jain and D. M. McDonald, *Am. J. Pathol.*, 2000, **156**, 1363–1380.
- 16 J. A. Nagy, S.-H. Chang, A. M. Dvorak and H. F. Dvorak, *Br. J. Cancer*, 2009, **100**, 865–869.
- 17 C. Franco and H. Gerhardt, *Nature*, 2012, **488**, 465–466.
- 18 P. Vaupel, F. Kallinowski and P. Okunieff, *Cancer Res.*, 1989, **49**, 6449–6465.
- 19 P. Vaupel and A. Mayer, *Cancer Metastasis Rev.*, 2007, **26**, 225–239.
- 20 J. C. Firrell, G. P. Lewis and L. J. F. Youlten, *Microvasc. Res.*, 1982, **23**, 294–310.
- 21 M. Inggrid Setyawati, C. Yong Tay, D. Docter, R. H. Stauber and D. Tai Leong, *Chem. Soc. Rev.*, 2015, **44**, 8174–8199.
- 22 H. Hashizume, P. Baluk, S. Morikawa, J. W. McLean, G. Thurston, S. Roberge, R. K. Jain and D. M. McDonald, *Am. J. Pathol.*, 2000, **156**, 1363–1380.
- 23 S. K. Hobbs, W. L. Monsky, F. Yuan, W. G. Roberts, L. Griffith, V. P. Torchilin and R. K. Jain, *Proc. Natl. Acad. Sci. U. S. A.*, 1998, **95**, 4607–4612.
- 24 H. Cabral, Y. Matsumoto, K. Mizuno, Q. Chen, M. Murakami, M. Kimura, Y. Terada, M. R. Kano, K. Miyazono, M. Uesaka, N. Nishiyama and K. Kataoka, *Nat. Nanotechnol.*, 2011, **6**, 815–823.
- 25 J. Hrkach, D. V. Hoff, M. M. Ali, E. Andrianova, J. Auer, T. Campbell, D. D. Witt, M. Figa, M. Figueiredo, A. Horhotá, S. Low, K. McDonnell, E. Peeke, B. Retnarajan, A. Sabnis, E. Schnipper, J. J. Song, Y. H. Song, J. Summa, D. Tompsett, G. Troiano, T. V. G. Hoven, J. Wright, P. LoRusso, P. W. Kantoff, N. H. Bander, C. Sweeney, O. C. Farokhzad, R. Langer and S. Zale, *Sci. Transl. Med.*, 2012, **4**, 128ra39.
- 26 M. A. Miller, S. Gadde, C. Pfirschke, C. Engblom, M. M. Sprachman, R. H. Kohler, K. S. Yang, A. M. Laughney, G. Wojtkiewicz, N. Kamaly, S. Bhonagiri, M. J. Pittet, O. C. Farokhzad and R. Weissleder, *Sci. Transl. Med.*, 2015, **7**, 314ra183.
- 27 D. Tsvirkun, A. Grichine, A. Duperray, C. Misbah and L. Bureau, *Sci. Rep.*, 2017, **7**, 45036.
- 28 R. K. Jain, L. L. Munn and D. Fukumura, *Nat. Rev. Cancer*, 2002, **2**, 266–276.
- 29 D. Fukumura, D. G. Duda, L. L. Munn and R. K. Jain, *Microcirculation*, 2010, **17**, 206–225.
- 30 D. T. Fisher, J. B. Muhitch, M. Kim, K. C. Doyen, P. N. Bogner, S. S. Evans and J. J. Skitzki, *Nat. Commun.*, 2016, **7**, 10684.
- 31 J. M. Rosano, N. Tousi, R. C. Scott, B. Krynska, V. Rizzo, B. Prabhakarpandian, K. Pant, S. Sundaram and M. F. Kiani, *Biomed. Microdevices*, 2009, **11**(5), 1051–1057.
- 32 A. C. Dudley, *Cold Spring Harbor Perspect. Med.*, 2012, **2**(3), a006536.
- 33 B. St Croix, C. Rago, V. Velculescu, G. Traverso, K. E. Romans, E. Montgomery, A. Lal, G. J. Riggins, C. Lengauer, B. Vogelstein and K. W. Kinzler, *Science*, 2000, **289**, 1197–1202.
- 34 S. L. Madden, B. P. Cook, M. Nacht, W. D. Weber, M. R. Callahan, Y. Jiang, M. R. Dufault, X. Zhang, W. Zhang, J. Walter-Yohrling, C. Rouleau, V. R. Akmaev, C. J. Wang, X. Cao, T. B. St Martin, B. L. Roberts, B. A. Teicher, K. W. Klinger, R.-V. Stan, B. Lucey, E. B. Carson-Walter, J. Laterra and K. A. Walter, *Am. J. Pathol.*, 2004, **165**, 601–608.
- 35 R. J. Buckanovich, D. Sasaroli, A. O'Brien-Jenkins, J. Botbyl, R. Hammond, D. Katsaros, R. Sandaltzopoulos, L. A. Liotta, P. A. Gimotty and G. Coukos, *J. Clin. Oncol.*, 2007, **25**, 852–861.
- 36 R. Bhati, C. Patterson, C. A. Livasy, C. Fan, D. Ketelsen, Z. Hu, E. Reynolds, C. Tanner, D. T. Moore, F. Gabrielli, C. M. Perou and N. Klauber-DeMore, *Am. J. Pathol.*, 2008, **172**, 1381–1390.
- 37 J.-L. Li and A. L. Harris, *Cancer Cell*, 2007, **11**, 478–481.
- 38 M. I. Bogorad, J. DeStefano, J. Karlsson, A. D. Wong, S. Gerecht and P. C. Searson, *Lab Chip*, 2015, **15**, 4242–4255.
- 39 W. Wu, C. J. Hansen, A. M. Aragón, P. H. Geubelle, S. R. White and J. A. Lewis, *Soft Matter*, 2010, **6**, 739–742.
- 40 J. M. Rosano, N. Tousi, R. C. Scott, B. Krynska, V. Rizzo, B. Prabhakarpandian, K. Pant, S. Sundaram and M. F. Kiani, *Biomed. Microdevices*, 2009, **11**, 1051–1057.
- 41 M. Sato, N. Sasaki, M. Ato, S. Hirakawa, K. Sato and K. Sato, *PLoS One*, 2015, **10**, e0137301.
- 42 J. Comelles, D. Caballero, R. Voituriez, V. Hortigüela, V. Wollrab, A. L. Godeau, J. Samitier, E. Martínez and D. Riveline, *Biophys. J.*, 2014, **107**, 1513–1522.
- 43 M.-H. Wu, S.-B. Huang and G.-B. Lee, *Lab Chip*, 2010, **10**, 939–956.
- 44 X.-Y. Wang, Y. Pei, M. Xie, Z.-H. Jin, Y.-S. Xiao, Y. Wang, L.-N. Zhang, Y. Li and W.-H. Huang, *Lab Chip*, 2015, **15**, 1178–1187.
- 45 Y. Zheng, J. Chen, M. Craven, N. W. Choi, S. Totorica, A. Diaz-Santana, P. Kermani, B. Hempstead, C. Fischbach-Teschl, J. A. López and A. D. Stroock, *Proc. Natl. Acad. Sci. U. S. A.*, 2012, **109**, 9342–9347.

- 46 A. W. Justin, R. A. Brooks and A. E. Markaki, *J. R. Soc., Interface*, 2016, **13**, 20160768.
- 47 T. Neumann, B. S. Nicholson and J. E. Sanders, *Microvasc. Res.*, 2003, **66**, 59–67.
- 48 A. Tourovskaya, M. Fauver, G. Kramer, S. Simonson and T. Neumann, *Exp. Biol. Med.*, 2014, **239**, 1264–1271.
- 49 Y. S. Zhang, M. Duchamp, R. Oklu, L. W. Ellisen, R. Langer and A. Khademhosseini, *ACS Biomater. Sci. Eng.*, 2016, **2**, 1710–1721.
- 50 I. S. Kinstlinger and J. S. Miller, *Lab Chip*, 2016, **16**, 2025–2043.
- 51 W. Zhu, X. Qu, J. Zhu, X. Ma, S. Patel, J. Liu, P. Wang, C. S. E. Lai, M. Gou, Y. Xu, K. Zhang and S. Chen, *Biomaterials*, 2017, **124**, 106–115.
- 52 J. Ribas, H. Sadeghi, A. Manbachi, J. Leijten, K. Brinegar, Y. S. Zhang, L. Ferreira and A. Khademhosseini, *Appl. In Vitro Toxicol.*, 2016, **2**, 82–96.
- 53 R. Devillard, E. Pagès, M. M. Correa, V. Kériquel, M. Rémy, J. Kalisky, M. Ali, B. Guillotin and F. Guillemot, *Methods Cell Biol.*, 2014, **119**, 159–174.
- 54 Y. C. Park, C. Zhang, S. Kim, G. Mohamedi, C. Beigie, J. O. Nagy, R. G. Holt, R. O. Cleveland, N. L. Jeon and J. Y. Wong, *ACS Appl. Mater. Interfaces*, 2016, **8**, 31541–31549.
- 55 A. Hasan, A. Paul, N. E. Vrana, X. Zhao, A. Memic, Y.-S. Hwang, M. R. Dokmeci and A. Khademhosseini, *Biomaterials*, 2014, **35**, 7308–7325.
- 56 X. Wang, D. T. T. Phan, D. Zhao, S. C. George, C. C. W. Hughes and A. P. Lee, *Lab Chip*, 2016, **16**, 868–876.
- 57 X. Wang, D. T. T. Phan, S. C. George, C. C. W. Hughes and A. P. Lee, *Lab Chip*, 2016, **16**, 282–290.
- 58 Y. C. Park, C. Zhang, S. Kim, G. Mohamedi, C. Beigie, J. O. Nagy, R. G. Holt, R. O. Cleveland, N. L. Jeon and J. Y. Wong, *ACS Appl. Mater. Interfaces*, 2016, **8**, 31541–31549.
- 59 M. Howard, B. J. Zern, A. C. Anselmo, V. V. Shuvaev, S. Mitragotri and V. Muzykantov, *ACS Nano*, 2014, **8**, 4100–4132.
- 60 A. Thomas, J. Tan and Y. Liu, *Microvasc. Res.*, 2014, **94**, 17–27.
- 61 T. Bhowmick, E. Berk, X. Cui, V. R. Muzykantov and S. Muro, *J. Controlled Release*, 2012, **157**, 485–492.
- 62 H. Klingberg, S. Loft, L. B. Oddershede and P. Møller, *Nanoscale*, 2015, **7**, 11409–11419.
- 63 N. Korin, M. Kanapathipillai, B. D. Matthews, M. Crescente, A. Brill, T. Mammoto, K. Ghosh, S. Jurek, S. A. Bencherif, D. Bhatta, A. U. Coskun, C. L. Feldman, D. D. Wagner and D. E. Ingber, *Science*, 2012, **337**, 738–742.
- 64 N. Doshi, B. Prabhakarpandian, A. Rea-Ramsey, K. Pant, S. Sundaram and S. Mitragotri, *J. Controlled Release*, 2010, **146**, 196–200.
- 65 P. Kolhar, A. C. Anselmo, V. Gupta, K. Pant, B. Prabhakarpandian, E. Ruoslahti and S. Mitragotri, *Proc. Natl. Acad. Sci. U. S. A.*, 2013, **110**, 10753–10758.
- 66 Y. Kim, M. E. Lobatto, T. Kawahara, B. L. Chung, A. J. Mieszawska, B. L. Sanchez-Gaytan, F. Fay, M. L. Senders, C. Calcagno, J. Becroft, M. T. Saung, R. E. Gordon, E. S. G. Stroes, M. Ma, O. C. Farokhzad, Z. A. Fayad, W. J. M. Mulder and R. Langer, *Proc. Natl. Acad. Sci. U. S. A.*, 2014, **111**, 1078–1083.
- 67 B. Prabhakarpandian, M.-C. Shen, J. B. Nichols, C. J. Garson, I. R. Mills, M. M. Matar, J. G. Fewell and K. Pant, *J. Controlled Release*, 2015, **201**, 49–55.
- 68 A. Albanese, A. K. Lam, E. A. Sykes, J. V. Rocheleau and W. C. W. Chan, *Nat. Commun.*, 2013, **4**, 2718.
- 69 D. Pozzi, G. Caracciolo, L. Digiocomo, V. Colapicchioni, S. Palchetti, A. L. Capriotti, C. Cavaliere, R. Z. Chiozzi, A. Puglisi and A. Laganà, *Nanoscale*, 2015, **7**, 13958–13966.
- 70 S. Palchetti, D. Pozzi, A. L. Capriotti, G. L. Barbera, R. Z. Chiozzi, L. Digiocomo, G. Peruzzi, G. Caracciolo and A. Laganà, *Colloids Surf., B*, 2017, **153**, 263–271.
- 71 K. Namdee, D. J. Sobczynski, P. J. Onyskiw and O. Eniola-Adefeso, *Bioconjugate Chem.*, 2015, **26**, 2419–2428.
- 72 A. Patra, T. Ding, G. Engudar, Y. Wang, M. M. Dykas, B. Liedberg, J. C. Y. Kah, T. Venkatesan and C. L. Drum, *Small*, 2016, **12**, 1174–1182.
- 73 L. G. Rigat-Brugarolas, A. Elizalde-Torrent, M. Bernabeu, M. D. Niz, L. Martin-Jaular, C. Fernandez-Becerra, A. Homs-Corbera, J. Samitier and H. A. del Portillo, *Lab Chip*, 2014, **14**, 1715–1724.
- 74 K. Rennert, S. Steinborn, M. Gröger, B. Ungerböck, A.-M. Jank, J. Ehgartner, S. Nietzsche, J. Dinger, M. Kiehntopf, H. Funke, F. T. Peters, A. Lupp, C. Gärtner, T. Mayr, M. Bauer, O. Huber and A. S. Mosig, *Biomaterials*, 2015, **71**, 119–131.
- 75 D. A. Reasor, M. Mehrabadi, D. N. Ku and C. K. Aidun, *Ann. Biomed. Eng.*, 2013, **41**, 238–249.
- 76 E. Carboni, K. Tschudi, J. Nam, X. Lu and A. W. K. Ma, *AAPS PharmSciTech*, 2014, **15**, 762–771.
- 77 R. D'Apolito, G. Tomaiuolo, F. Taraballi, S. Minardi, D. Kirui, X. Liu, A. Cevenini, R. Palomba, M. Ferrari, F. Salvatore, E. Tasciotti and S. Guido, *J. Controlled Release*, 2015, **217**, 263–272.
- 78 A. J. Thompson and O. Eniola-Adefeso, *Acta Biomater.*, 2015, **21**, 99–108.
- 79 A. Thomas, J. Tan and Y. Liu, *Microvasc. Res.*, 2014, **94**, 17–27.
- 80 Y. Kim, M. E. Lobatto, T. Kawahara, B. L. Chung, A. J. Mieszawska, B. L. Sanchez-Gaytan, F. Fay, M. L. Senders, C. Calcagno, J. Becroft, M. T. Saung, R. E. Gordon, E. S. G. Stroes, M. Ma, O. C. Farokhzad, Z. A. Fayad, W. J. M. Mulder and R. Langer, *Proc. Natl. Acad. Sci. U. S. A.*, 2014, **111**, 1078–1083.
- 81 S. Palchetti, D. Pozzi, A. L. Capriotti, G. L. Barbera, R. Z. Chiozzi, L. Digiocomo, G. Peruzzi, G. Caracciolo and A. Laganà, *Colloids Surf., B*, 2017, **153**, 263–271.
- 82 R. D'Apolito, G. Tomaiuolo, F. Taraballi, S. Minardi, D. Kirui, X. Liu, A. Cevenini, R. Palomba, M. Ferrari, F. Salvatore, E. Tasciotti and S. Guido, *J. Controlled Release*, 2015, **217**, 263–272.
- 83 A. Skardal, T. Shupe and A. Atala, *Drug Discovery Today*, 2016, **21**, 1399–1411.
- 84 N. J. Schork, *Nature*, 2015, **520**, 609.
- 85 S. W. Hell, S. J. Sahl, M. Bates, X. Zhuang, R. Heintzmann, M. J. Booth, J. Bewersdorf, G. Shtengel, H. Hess, P. Tinnefeld, A. Honigmann, S. Jakobs, I. Testa, L. Cognet, B. Lounis, H. Ewers, S. J. Davis, C. Eggeling, D. Klenerman,

- K. I. Willig, G. Vicidomini, M. Castello, A. Diaspro and T. Cordes, *J. Phys. D: Appl. Phys.*, 2015, **48**, 443001.
- 86 R. M. Power and J. Huisken, *Nat. Methods*, 2017, **14**, 360–373.
- 87 S. Reardon, *Nature*, DOI: 10.1038/nature.2017.21818.
- 88 A. Junaid, A. Mashaghi, T. Hankemeier and P. Vulto, *Curr. Opin. Biomed. Eng.*, DOI: 10.1016/j.cobme.2017.02.002.